

Article

The Formation and Application of Submicron Spherical BaTiO₃ Particles for the Diffusion Layer of Medical Dry Films

Baodan Zhang , Haibo Jin * , Xu Liu , Xiaoyan Guo, Guangxiang He  and Suohe Yang

Beijing Key Laboratory of Fuels Cleaning and Advanced Catalytic Emission Reduction Technology, College of Chemical Engineering, Beijing Institute of Petrochemical Technology, Beijing 102617, China; zbd330@foxmail.com (B.Z.); liuxu@bipt.edu.cn (X.L.); guoxiaoyan@bipt.edu.cn (X.G.); hgx@bipt.edu.cn (G.H.); yangsuohe@bipt.edu.cn (S.Y.)

* Correspondence: jinhaibo@bipt.edu.cn; Tel.: +86-10-81292208

Received: 10 October 2019; Accepted: 11 November 2019; Published: 14 November 2019



Abstract: Submicron spherical barium titanate (BaTiO₃) was prepared by batch precipitation in an alkaline solution of a BaCl₂–TiCl₄–NaOH reaction system. The influence of various parameters on the morphology of BaTiO₃ powders was investigated in this study. Spherical BaTiO₃ particles can be obtained by reacting for 20 min, which was used to prepare the dry sheet of a medical dry chemical reagent. The morphology of the particles was affected by the stirring speed and the alkaline concentration; the particle size decreased as the stirring speed increased. The hydroxyl ion in the solution acts as a catalyst that can promote the formation of spherical BaTiO₃. The formation mechanism of the BaTiO₃ sphere is proposed to have three steps: the formation of a Ba–Ti gel and nucleation, self-combination/growth of the BaTiO₃ crystal nucleus, and Ostwald ripening. In addition, it is feasible to apply the prepared BaTiO₃ sphere to medical dry chemical detection reagents.

Keywords: spherical BaTiO₃; preparation; formation mechanism; medical applications

1. Introduction

In recent decades, barium titanate (BaTiO₃) with a perovskite structure has been widely applied to multilayer ceramic capacitors (MLCCs), gate dielectrics, and embedded capacitors in printed circuit boards due to its good ferroelectric properties and high dielectric constant [1]. As a piezoelectric material, BaTiO₃ can also be made for transducers and actuators [2]. When doped with other elements, its semiconducting properties have a positive temperature coefficient of resistivity (PTCR) [3]. In addition, the surface sensitivity of BaTiO₃ to gas adsorption can be used for chemical sensors [4]. In recent years, some researchers have pointed out that BaTiO₃ can be used in medical bone transplantation [5]. Moreover, BaTiO₃ also has optical characteristics such as high whiteness and high reflectivity, similar to TiO₂ and BaSO₄. These properties can be applied in medical dry chemical detection reagents [6,7], which can detect health indicators quickly. This represents a potential research direction for barium titanate materials.

Generally, medical reagent dry sheets can be divided into three layers: a support layer, a reagent layer, and a diffusion layer. The main functions of the diffusion layer are to filter, permeate, diffuse, reflect, etc.; the analyte can permeate and diffuse evenly into the reagent layer and react with the matrix. In addition, the diffusion layer plays a role in the reflection of light. The greater the reflectivity, the less the liquid to be tested is affected by the color of the dry film, and the more accurate the concentration of the liquid is. Therefore, the performance of the diffusion layer depends to a great extent on its composition. The preparation of spherical, uniform BaTiO₃ particles is an important step toward the fabrication of a diffusion layer in medical dry films.

The preparation of BaTiO₃ particles and the synthesis of specific particles have been extensively investigated over the last 20 years; more than 100 papers on the subject are available in the published literatures. In addition to the solid phase method, there are various wet chemical methods, including the hydrothermal method [8,9], the sol-gel method [10], the precipitation method [11], spray pyrolysis [12], and techniques using a combination of conventional methods, such as the sol-precipitation method, the sol-hydrothermal method, and so on [13,14]. In recent years, with the development of new wet chemical methods and the introduction of new technologies, new wet chemical combination methods are able to produce relatively regular spherical BaTiO₃; these include the microemulsion method, the Pechini method, sonochemical synthesis, the microwave-hydrothermal method, and so on [15–18]. The uniformity and dispersibility of BaTiO₃ particles can be improved by using a modified preparation technology, but the operation process is quite complicated and thus not conducive to industrialization and expansion of production. Traditional preparation methods also have their own advantages and disadvantages [19]. The powders obtained by the hydrothermal method have a uniform particle size and chemical composition, but have some defects, such as the formation of agglomerates during the reaction, and high requirements for equipment that must withstand high temperature and pressure conditions during the procedure. The products prepared by the sol-gel method have high purity, high dispersibility, and easy control of product components, but the high raw material cost and low yield are shortcomings of this method that affect its viability in industrial applications.

The precipitation method has interested researchers in recent years due to its simple operation process, low raw material cost, short reaction cycle, and so on [20–22]. Testino studied the kinetic formation mechanism of BaTiO₃ particles by the precipitation method, established a kinetic model, and analyzed the effects of barium concentration, reaction temperature, and Ba/Ti ratio on kinetics and crystal size from the perspective of nucleation and crystal growth [23,24]. Viviani et al. studied the relationship between concentration and the formation of BaTiO₃ by a direct precipitation method, using TiCl₄ and Ba(OH)₂ as raw materials [25]. Although the preparation of BaTiO₃ by precipitation has been studied for many years, there is little information on the effect of reaction time, alkalinity, stirring speed, and other parameters of the reaction system on the particle size of spherical BaTiO₃, and the formation mechanism of the BaTiO₃ sphere has rarely been analyzed in detail.



To gain further understanding of the formation process of BaTiO₃ sphere in the reaction system, the synthesis of BaTiO₃ spheres was conducted by a batch precipitation method based on the investigation of various factors, with a reaction temperature below 100 °C. Equations (1) and (2) combine nucleation and crystal growth from the perspective of crystallization chemistry. Furthermore, the prepared products were applied to the diffusion layer of medical dry sheets to facilitate the detection and analysis of dry chemical reagents; this provides more selective space for the materials in the application field.

2. Materials and Methods

2.1. Materials

Titanium tetrachloride (A.R., 99.0%, Shanghai Maclean Biochemical Technology Co. Ltd., Beijing, China), barium chloride dihydrate (A.R., ≥99.5%, Sinopharm Chemical Reagent Co., Ltd., Beijing, China), NaOH (A.R., ≥96.0%, Beijing Chemical Plant, Beijing, China), and commercially available BaTiO₃ (A.R., Maclean Biotechnology Co. Ltd., Beijing, China) were the main materials.

2.2. Synthesis Methods

A sample of spherical BaTiO₃ with a uniform particle size was prepared by the batch precipitation method. Titanium tetrachloride was dropped slowly into ice-cooled (below 10 °C) deionized water under stirring, and after hydrolyzing this solution was regarded as the Ti source. At the same time, barium chloride dihydrate was dissolved in 60 mL deionized water using R (the ratio of Ba/Ti) = 1.11, which was used as the Ba solution. An excess of Ba was used compared with the stoichiometric amount, which had a great influence on the reaction kinetics [11]. The above two solutions were then mixed to form a Ba–Ti solution. The acidic Ba–Ti solution was mixed with an equal amount of 0.6–1.2 M NaOH solution in a 500-mL four-necked flask (the concentration was calculated according to the total volume after the reaction of the mixed solution). The concentration of Ba in the reaction system was 0.1 M. The experiment was conducted for a reaction time of 5–180 min at a stirring speed of 250–1000 r/min. A white precipitate was obtained when the temperature was close to 90 °C.

The as-prepared product after aging was centrifuged, washed, and dried at 80 °C. The suspension was washed with an ammonia solution (pH: 10.0–10.2) to avoid having chloride ions in the products and reduce the leaching of Ba²⁺ from the surface of BaTiO₃ particles [19,26]. The reaction system was carried out under N₂ protection to avoid the introduction of CO₂.

2.3. The Preparation of Diffusion Layer of Dry Chemical Reagents

One gram of homemade BaTiO₃ (prepared by the above synthesis method) or commercially available BaTiO₃ was added (as a comparison) to the Erlenmeyer flask along with 1 mL of acetone solution, an appropriate amount of cellulose acetate solution (CA, Sinopharm Chemical Reagent Co., Ltd, Beijing, China), and trace surfactant, which can be used as the diffusion layer slurry. Then, the mixture was magnetically stirred for a certain period of time, and coated on the fixed dry reagent layer by a coating machine. The coated layer was dried at room temperature to obtain a BaTiO₃ diffusion layer that can be used for in vitro diagnostic reagents in a dry chemical.

2.4. Characterization

The phase of the as-prepared samples was analyzed by X-ray powder diffraction (Rigaku Max-2600, Japanese Neo-Confucianism Co. LTD, Tokoy, Japan) at room temperature and with the conditions of 40 kV tube voltage and 30 mA tube current (Cu K α). In addition, the morphology of the particles was investigated by field-emission scanning electron microscopy (FE-SEM, ZEISS-SUPRA 55, Carl Zeiss AG, Jena, Germany). The particle size distribution was measured by a laser particle size analyzer PSD (Rise-2008, Jinan Runzhi Technology Co., Ltd., Jinan, China).

3. Results and Discussion

3.1. The Effect of Reaction Time

In this study, the effect of reaction time on the as-prepared BaTiO₃ powders was investigated. During the course of the experiment, white precipitations were collected using a centrifuge tube after 5, 20, 90, and 180 min of reaction time (time 0 corresponds to the moment the temperature in the mixed solution reaches the given reaction temperature).

The X-ray diffraction (XRD) patterns of BaTiO₃ obtained at different reaction times are shown in Figure 1. The XRD pattern of the sample reacted for 5 min shows a BaTiO₃ peak. The peak intensity of the as-prepared powder for 20 min is a little more noticeable in the XRD pattern. In addition, it lessens a bit with a further increase in reaction time. It is worth noting that the reaction was completed within several minutes at a temperature of 90 °C for a raw material concentration of 0.1 M. Testino and Viviani [11,25] have also reported that the reaction solution can rapidly form a BaTiO₃ crystal nucleus at T = 82–92 °C in a suitable concentration range, and the concentration can be lower with increasing temperature. The effect of the concentration on the particle size and crystallite size of BaTiO₃ has been described in a previous study [11]. The change in concentration had no significant effect on

the XRD diffraction peak of the BaTiO_3 , but the particle size was reduced appropriately. A low Ba^{2+} concentration of 0.1 M was selected in this study for various reasons. First, the larger BaTiO_3 particles obtained at this concentration can be used better to the dry diffusion layer in comparison with those at a high concentration. Second, lower concentrations lengthen the reaction time, thereby prolonging the reaction cycle and increasing the costs. The yield of powders at this concentration can be over 99%.

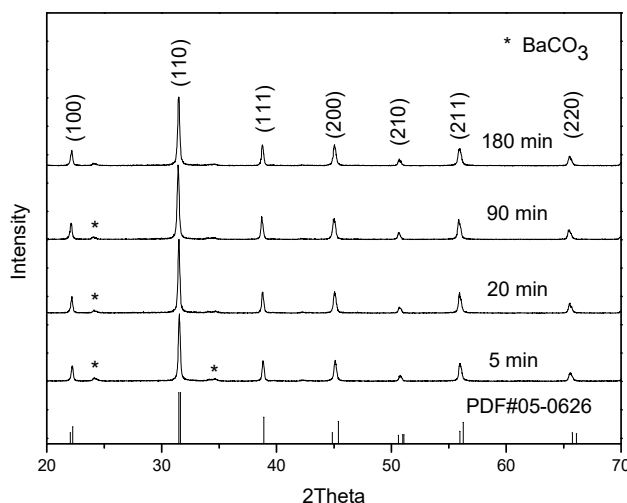


Figure 1. XRD patterns of BaTiO_3 particles prepared at $90\text{ }^\circ\text{C}$.

As shown in Figure 1, there was a splitting of the diffraction lines at 2θ angles, which was in accordance with the JCPDS card No. 05-0626, demonstrating that the products synthesized at $90\text{ }^\circ\text{C}$ consisted of pseudo tetragonal crystals. Moreover, the powders prepared by the batch precipitation method were obtained without calcination, which reduced the equipment cost and is advantageous for industrial production. This also rendered it easy to apply to the medical dry chemical diffusion layer. Generally, the common tetragonal structure of BaTiO_3 was obtained after heating treatment at more than $1100\text{ }^\circ\text{C}$. The phenomenon in this study can be contributed to particle coarsening or removal of hydroxyl groups from the perovskite lattice [25,27].

3.2. The Effect of Stirring Speed

The effects of stirring speed on solutions were examined by adding powders to solutions under a concentration of 0.1 M BaCl_2 and 20 min reaction time. The stirring speed varied from 100 rpm to 1000 rpm. Some examples of the morphology of as-prepared particles are presented in Figure 2. The particle size was uneven and there was adhesion between the particles when the rotation speed was lower than 250 rpm. From the perspective of particle uniformity, the distribution of particles tended to be more uniform and the formative particle gradually became complete as the stirring speed increased. As can be seen in Figure 2C, the surface of BaTiO_3 particles obtained at 700 rpm was relatively smooth, and the particle morphology was somewhat spherical. Below this rotation speed, it was obvious that the particles were not completely formed and that there were many defects on the surface of the particles. Above this rotation speed, spherical particles adhered to other small particles, while the particle size was similar to that of 700 rpm.

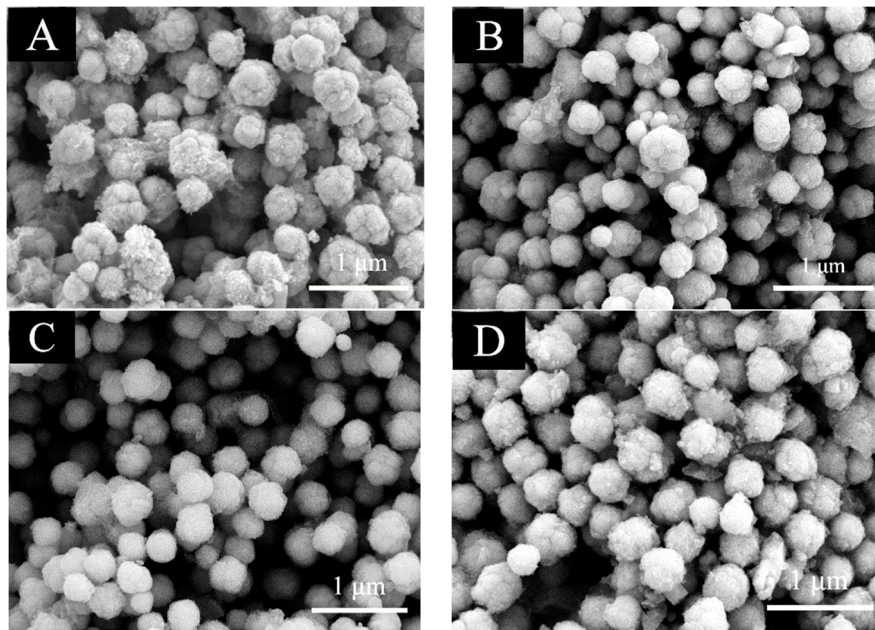


Figure 2. Morphology of BaTiO₃ powders synthesized at different stirring speeds: (A) 100 rpm, (B) 250 rpm, (C) 700 rpm, (D) 1000 rpm.

It has been reported in the literature [28,29] that the stirring speed in the reaction system and the particle size of prepared powders have a certain qualitative relationship. The particle size tended to decrease with increasing agitation speed (Figure 2), which is consistent with the results reported in the literature [30]. As the stirring speed increased, the frequency of collision among molecules and the formation of crystal nuclei in the solution increased, corresponding to the nucleation theory, and the solution was uniformly mixed, which was favorable for the uniform growth of individual crystal particles. In addition, there were several small particles on the surface of the large particle in Figure 2D. Due to the coalescence mechanism, the large particles gradually became larger by aggregating the smaller particles.

The dependence of the particle size distribution on the stirring speed is indicated in Figure 3 based on measurements from a Rise-2008 laser particle size analyzer. There was one particle size centered at 200 nm and a weak shoulder at 35 nm. Moreover, this value was in agreement with that calculated by the Scherrer formula from the diffraction data, which provided valuable data on crystal growth mechanism and aggregation. It also showed that the average particle size of the powders changed little when increasing the stirring speed from 100 to 1000 rpm. The distribution of particle size gradually narrowed with the increase in stirring speed. In addition, when the rotational speed was increased to 1000 rpm, the particle size distribution tended to broaden. This is for two reasons. From a macroscopic point, as the stirring speed increased, the BaTiO₃ particles formed by small crystallites were easily ejected at high speeds as the blades rotated at high speed. On the other hand, from a microscopic point of view, the shearing force generated by the rotation of the blade during the high rotation speed was large [29], and the BaTiO₃ submicron sphere formed in the solution was broken, so several small particles attached to the surface of the BaTiO₃ sphere were dispersed in the solution and further crystal growth was carried out by secondary nucleation. Accordingly, in addition to the original relatively complete BaTiO₃ particles in the solution, there were small particles formed by secondary nucleation, resulting in a relatively wide particle size at 1000 rpm.

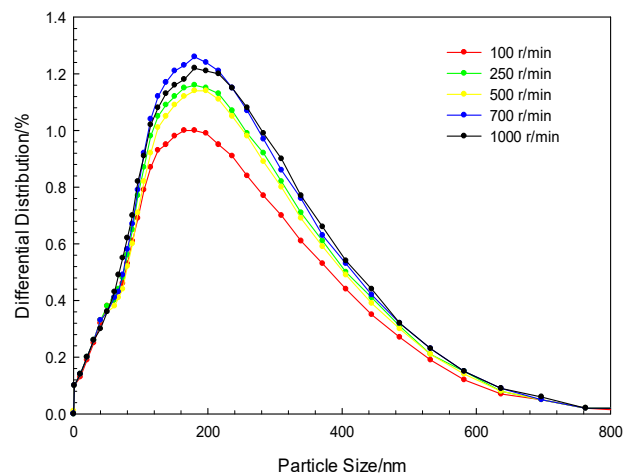


Figure 3. Distributions of particle size obtained at different stirring speeds.

3.3. Effect of Concentration of NaOH

The morphology of the obtained powders at different concentrations of NaOH is presented in Figure 4. When the NaOH concentration increased from 0.6 M to 0.8 M, the resulting product grew from an irregular morphology to a spherical shape with severe defects. With an increase in alkali concentration to 1.0 M, the prepared BaTiO₃ powder had a relatively regular spherical shape under scanning electron microscopy. Because of the uniform spherical shape, it was better applied to the dry chemical diffusion layer; the particles were uniformly diffused through the diffusion layer onto the reagent layer for substrate reaction. As the concentration of OH⁻ ions continued to increase from 1.0 M to 1.2 M, the spherical particle size decreased from 200 nm to 150 nm, which was in accordance with the results from Hwang, Wang, etc. [10,14,31]. The OH⁻ taken as a catalyst in the solution maintained the supersaturation of the reaction system to complete the precipitation reaction, thereby promoting the formation of BaTiO₃ crystallites. In addition to the alkaline environment being essential for producing a stable barium titanate particle, it can also serve as a growth inhibitor, preventing further growth and agglomeration of the product, which agrees with the description of nucleation theory [32].

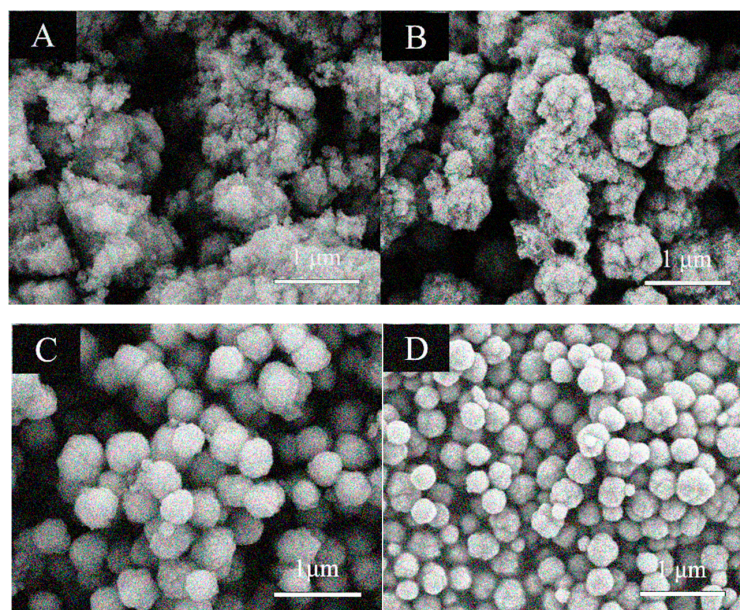


Figure 4. Morphology of BaTiO₃ powders synthesized at different concentrations of NaOH: (A) 0.6 M, (B) 0.8 M, (C) 1.0 M, (D) 1.2 M.

3.4. The Formation Mechanism of Spherical BaTiO₃

Submicron spherical BaTiO₃ particles were successfully obtained at a low Ba ion concentration of 0.1 M using a batch precipitation method. It was found that the formation of BaTiO₃ precipitates can be processed by two steps. First, the amorphous colloidal liquid rapidly formed a Ti-rich gel phase under the heat of reaction between acid and alkali after the Ba–Ti solution was mixed with the NaOH solution at room temperature. Next, the reaction of the gel phase with Ba²⁺ or BaOH⁺ in the solution proceeded during the gradual warming to form a white precipitate suspension that contained BaTiO₃. All steps of the reaction were carried out under stirring.

The mechanism of BaTiO₃ formation has also been reported in the literature [9,21,23,31,33,34]. Testino et al. [23] analyzed the formation of barium titanate from the perspective of crystal nucleation and growth. The kinetic analysis of crystallization of hydrothermal BaTiO₃ was studied by Özen et al. [9]. The formation process of spherical BaTiO₃ particles has rarely been analyzed in detail.

The formation mechanism of spherical BaTiO₃ particles was identified in this study. It is divided into three steps. In the initial stage of the reaction, the Ba–Ti solution is rapidly mixed with the NaOH solution at room temperature to form a Ti-rich gel phase [23]. The barium-containing ions (Ba²⁺ or BaOH⁺) diffuse into the Ti-rich gel phase to form a Ba–Ti gel, and then form a BaTiO₃ nucleus by the catalyzing of OH[−] under a thermal field, corresponding to stage (i) in Figure 5.

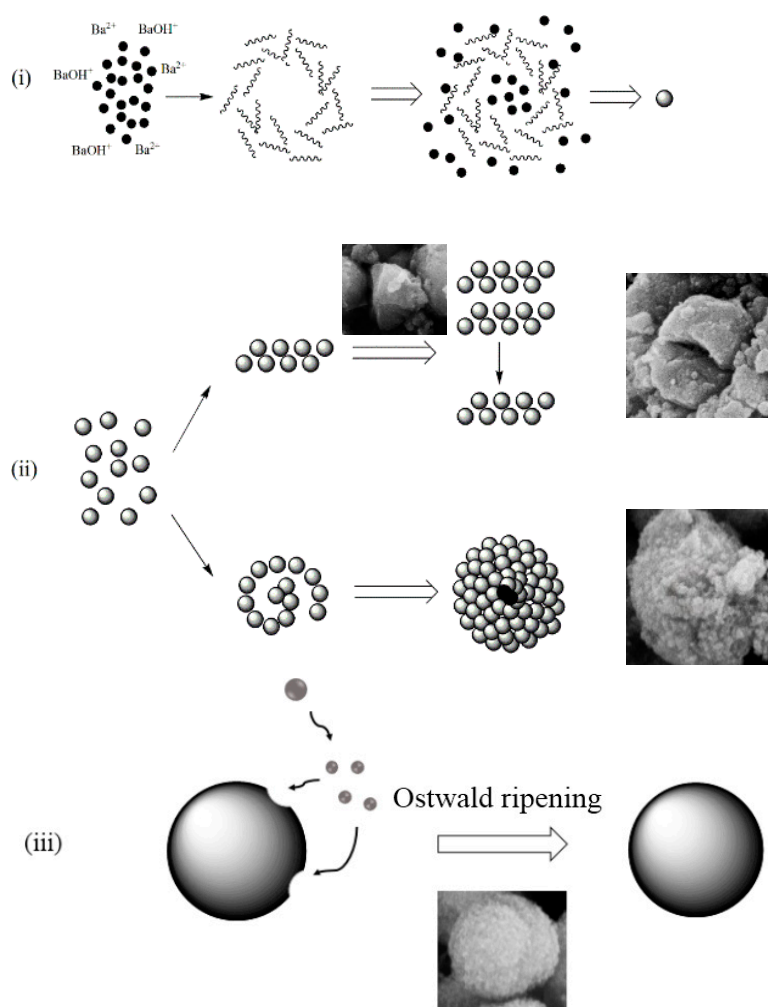


Figure 5. Formation mechanism diagram of BaTiO₃ sphere: (i) The initial stage of the reaction; (ii) The self-combination/growth of a crystal nucleus; (iii) Ostwald ripening.

The second stage is the self-combination/growth of a crystal nucleus, which can be accomplished in two ways: (a) BaTiO₃ crystallites can self-assemble to form flaky grains, which are further overlaid onto spherical BaTiO₃, as seen in Figure 5(ii). (b) The spherical BaTiO₃ may also be formed by screw dislocation [35]. The middle point is the spiral dislocation outcrop growth hill. The growth trajectory of the crystal was spiral, corresponding to the stage of Figure 5(ii).

From the perspective of crystal chemistry, the interface formed by the BaTiO₃ crystal was composed of a negative ion coordination polyhedron [36], that is, Ba was located at the center of eight octahedral structures composed of Ti and O. Its crystal orientation played a significant role in the morphology of the crystal. Generally, the negative ion coordination polyhedron has the fastest crystal growth rate, corresponding to the apex angle, and often disappears. Growth primitives composed of different connection forms have different stability energies [37]. During the course of the reaction, the BaTiO₃ crystals were oriented in a certain arrangement due to the electrostatic action, and most of them were combined by an apex angle connection. The high stability of the elements formed by the apex angle connection was attributed to this event.

The screw dislocation outcrop existing on the crystal plane in the screw dislocation growth mechanism (BCF theoretical model) was used as a source for crystal growth and acted as a catalyst to prompt the growth of a BaTiO₃ crystal nucleus. Zhong et al. [38] studied the crystal structure of silicon carbide according to the negative ion coordination polyhedron growth primitive model, showing that the growth element tetrahedron dislocation occurred along an axis when it was superposed on the crystal plane, and that it was in a spiral path. The BCF theoretical model can be used to explain the growth of many actual crystals [39].

The last stage is the Ostwald ripening, based on the existent BaTiO₃ sphere. The growth of BaTiO₃ particles tended to be complete under Ostwald ripening, and the surface was smoother, corresponding to the stage of Figure 5(iii). The large particles gradually grew further with the influence of interface energy, resulting in the smoother surface of the defective particles.

3.5. The Application of As-Prepared Powders on the Medical Dry Chemical Diffusion Layer

BaTiO₃ powder was used for the preparation of a dry chemical diffusion layer. It was stirred for a certain time to coat a relatively smooth diffusion layer. It can be interpreted as follows. Adhesive cellulose acetate (CA) took some time to dissolve in the solution and uniformly wrap the barium titanate particles. When the stirring time was too short, some of the undissolved particles were dispersed in the slurry, resulting in a rough surface of the diffusion layer. As the stirring time was extended, CA gradually dissolved to obtain a smooth diffusion layer. It is undeniable that the smoother diffusion layer is better for use in medical dry chemical reagents.

A comparison between commercial BaTiO₃ and as-prepared samples is shown in Figure 6. The self-made BaTiO₃ in the wavelength range of 400–850 nm had higher light reflectivity than the commercially available BaTiO₃ in Figure 6a. The reflectivity of the commercially available BaTiO₃ had the value of 91.1% at 550–850 nm, while that of the self-made BaTiO₃ was more than 99.2%, which represented a significant advantage in comparison with TiO₂ or BaSO₄ having been applied to the medical dry chemical reagent film (Figure 7).

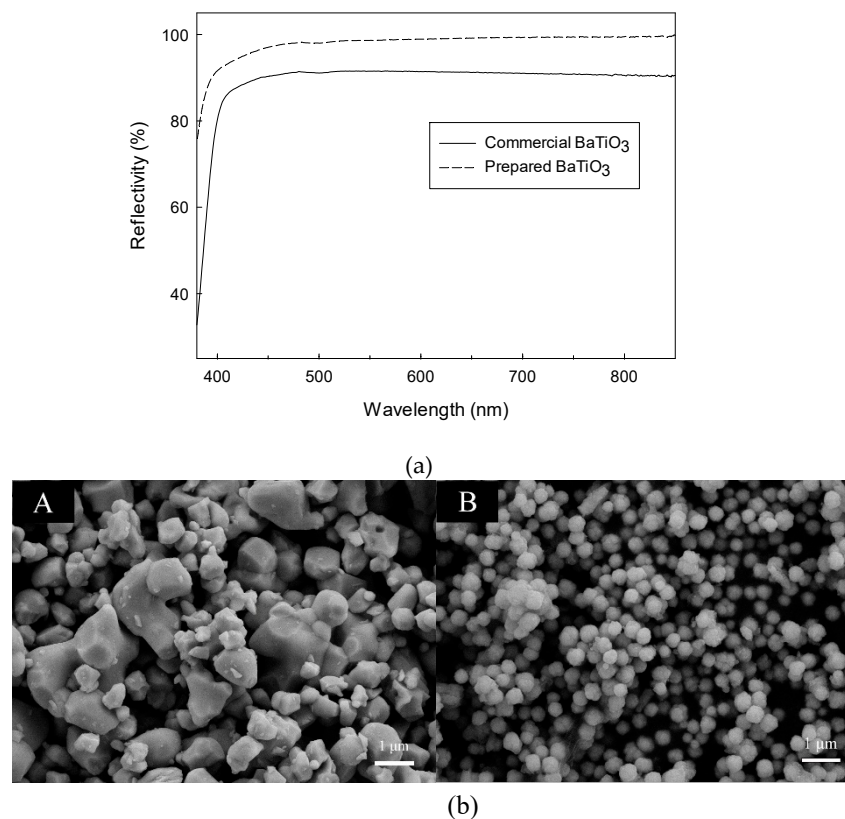


Figure 6. (a) Reflectivity of different BaTiO₃ samples in the experiment. (b) Morphology of commercial BaTiO₃ and as-prepared samples: (A) Commercial BaTiO₃; (B) Prepared BaTiO₃.

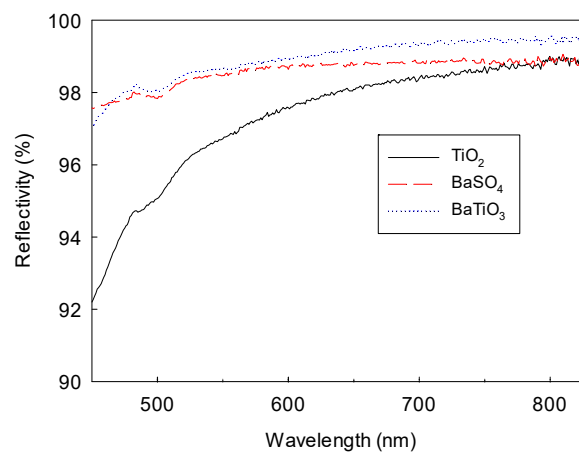


Figure 7. Comparison of light reflectance of raw materials prepared by different diffusion layers.

From the prospective of morphology, the commercially available BaTiO₃ particles had inhomogeneous particle sizes and irregular shapes, while the self-made BaTiO₃ particles had a more regular spherical shape, more uniform particle size, and more uniform distribution relative to the commercially available BaTiO₃ (as shown in Figure 6b). The interfering substances were filtered out when serum was dripped into the diffusion layer, which could be uniformly dispersed into the reagent layer to provoke a uniform color reaction, so that the concentration of the analyte was determined by a color test to achieve reagent detection. However, the diffusion layer obtained by the commercially available BaTiO₃ had a nonuniform void, and it was difficult for the serum to uniformly permeate due to the capillary phenomenon of the pores in the diffusion layer after dripping, resulting in uneven color development and affecting the testing effect. Meanwhile, the spherical BaTiO₃ particles prepared

by the batch precipitation method herein had good repeatability in applications with medical dry chemical reagents (as shown in Figure 8).

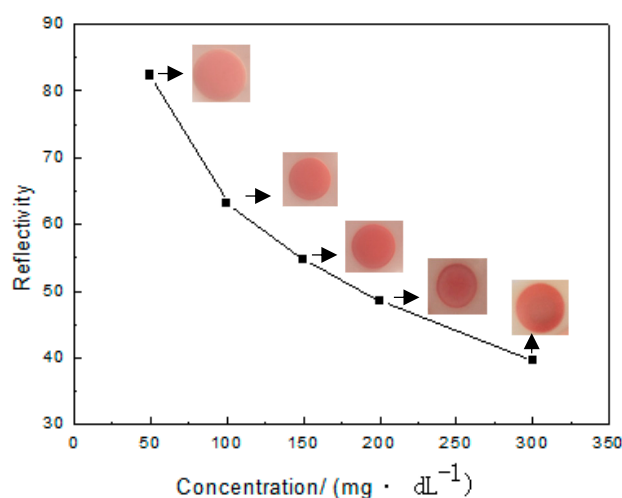


Figure 8. Reflectivity and color images at different concentrations of serum reaction.

The relationship between reflectivity and color images at different serum concentrations is shown in Figure 8. As the concentration increased, the color reaction was much more evident: the red was deeper, resulting in a decrease in the corresponding light reflectance value. When the concentration of the serum was higher, the absorbance of light at a wavenumber of 740 nm (red) improved. It turned out that the intensity of light reflected in the detector decreased, demonstrating that the reflectivity was low. At a low concentration the situation was the opposite.

4. Conclusions

Submicron spherical BaTiO₃ was synthesized by batch precipitation via a BaCl₂-TiCl₄-NaOH reaction system. The effects of different conditions, such as reaction time, stirring speed, and alkali concentration, on the morphology of the BaTiO₃ powder was analyzed. It was found that a good spherical BaTiO₃ can be synthesized by reacting in an alkaline system for 20 min, which saves preparation time for the dry sheet of a medical dry chemical reagent. It was also found that the morphology of the powders will be affected by the stirring speed, and that the particle size will decrease with an increase in the stirring speed. Hydroxyl ions in the solution, in addition to providing an alkaline environment during the reaction to form BaTiO₃ crystals, acted as a catalyst to promote the progress of the reaction. In the present case, the formation of spherical BaTiO₃ particles was achieved in three steps: the formation of a Ba-Ti gel and nucleation, self-combination/growth of BaTiO₃ crystal nucleus, and Ostwald ripening. In addition, BaTiO₃ powders prepared in this study were applied to the preparation of dry chemical reagent detection sheets. The results showed that the color reaction was obviously improved as compared to a commercial sample, and the reaction process was reproducible.

Author Contributions: B.Z., H.J., and X.L. conceived and designed the experiments; B.Z. and X.L. performed the experiments; B.Z., X.G., and G.H. analyzed the data; S.Y. contributed materials; B.Z. and H.J. wrote the paper.

Funding: This study was supported by the National Natural Science Foundation of China (91634101) and The Project of Construction of Innovative Teams and Teacher Career Development for Universities and Colleges under Beijing Municipality (IDHT20180508).

Acknowledgments: The study was completed at the Beijing Key Laboratory of Fuels Cleaning and Advanced Catalytic Emission Reduction Technology, Beijing Institute of Petrochemical Technology. The authors wish to thank Ruiqi Li for his guidance in the field-emission scanning electron microscopy at the Institute of Automation Chinese Academy of Sciences.

Conflicts of Interest: The authors declare no potential conflicts of interest with respect to the research, authorship, and/or publication of this article.

References

1. Kwei, G.H.; Lawson, A.C.; Billinge, S.J.L.; Cheong, S.W. Structures of the ferroelectric phases of barium titanate. *J. Phys. Chem.* **1993**, *97*, 2368–2377. [[CrossRef](#)]
2. Buchal, C.; Siegert, M. Ferroelectric thin films for optical applications. *Integr. Ferroelectr.* **2001**, *35*, 1731–1740. [[CrossRef](#)]
3. Alles, A.B.; Burdick, V.L. Grain boundary oxidation in PTCR barium titanate thermistors. *J. Am. Ceram. Soc.* **1993**, *76*, 401–408. [[CrossRef](#)]
4. Nishizawa, H.; Katsube, M. Preparation of BaTiO₃ thin films using glycolate precursor. *J. Solid State Chem.* **1997**, *131*, 43–48. [[CrossRef](#)]
5. Vouilloz, F.J.; Castro, M.S.; Vargas, G.; Gorustovichb, A.; Fanovich, M.A. Reactivity of BaTiO₃-Ca₁₀(PO₄)₆(OH)₂ phases in composite materials for biomedical applications. *Ceram. Int.* **2017**, *43*, 4212–4221. [[CrossRef](#)]
6. Guo, X.; Li, Y.; Zheng, Y.; Cheng, P.; He, G. Synthesis and characterization of homogeneous titanium dioxide microspheres. *Fine Chem.* **2017**, *34*, 1404–1411.
7. Liu, Y.J.; Guo, X.; Gu, Q.; He, G.; Yang, S.; Jin, H. Formation and application of high reflectivity controllable barium sulfate microspheres. *Crystals* **2018**, *8*, 333. [[CrossRef](#)]
8. Kothandan, D.; Kumar, R.J.; Naidu, K.C.B. Barium titanate microspheres by low temperature hydrothermal method: Studies on structural, morphological, and optical properties. *J. Asian Ceram. Soc.* **2018**, *6*, 1–6. [[CrossRef](#)]
9. Özen, M.; Mertens, M.; Snijkers, F.; Cool, P. Hydrothermal synthesis and formation mechanism of tetragonal barium titanate in a highly concentrated alkaline solution. *Ceram. Int.* **2016**, *42*, 10967–10975. [[CrossRef](#)]
10. Hwang, U.Y.; Park, H.S.; Koo, K.K. Low-temperature synthesis of fully crystallized spherical BaTiO₃ particles by the Gel–Sol method. *J. Am. Ceram. Soc.* **2004**, *87*, 2168–2174. [[CrossRef](#)]
11. Testinon, A.; Buscaglia, M.T.; Viviani, M.; Buscaglia, V.; Nanni, P. Synthesis of BaTiO₃ particles with tailored size by precipitation from aqueous solutions. *J. Ceram. Soc.* **2004**, *87*, 79–83. [[CrossRef](#)]
12. Xu, H.R.; Gu, H.C.; Gao, L.; Guo, J.K. Preparation and characterization of spherical, solid barium titanate ultrafine powders with uniform composition by spray hydrolysis reaction. *J. Inorg. Mater.* **2002**, *17*, 938–944. [[CrossRef](#)]
13. Fan, G.N.; Huangpu, L.X.; He, X.G. Synthesis of single-crystal BaTiO₃ nanoparticles via a one-step sol-precipitation route. *J. Cryst. Growth* **2005**, *279*, 489–493. [[CrossRef](#)]
14. Wang, W.; Cao, L.; Liu, W.; Su, G.; Zhang, W. Low-temperature synthesis of BaTiO₃ powders by the sol-gel-hydrothermal method. *Ceram. Int.* **2013**, *39*, 7127–7134. [[CrossRef](#)]
15. Wang, J.; Fang, J.; Ng, S.C.; Gan, L.M.; Chew, C.H.; Wang, X.; Shen, Z. Ultrafine barium titanate powders via microemulsion processing routes. *J. Am. Ceram. Soc.* **2010**, *82*, 873–881. [[CrossRef](#)]
16. Prado, L.R.; De Resende, N.S.; Silva, R.S.; Egues, S.M.S.; Salazar-Banda, G.R. Influence of the synthesis method on the preparation of barium titanate nanoparticles. *Chem. Eng. Process. Process. Int.* **2016**, *103*, 12–20. [[CrossRef](#)]
17. Vuttivong, S.; Niemcharoen, S.; Seeharaj, P.; Vittayakorn, W.C.; Vittayakorn, N. Sonochemical synthesis of spherical BaTiO₃ nanoparticles. *Ferroelectrics* **2013**, *457*, 44–52. [[CrossRef](#)]
18. Xu, L. Preparation and Characterization of Barium Titanate Powders by Microwave-Assisted Sol-Hydrothermal Method. Master's Thesis, Nanjing University of Aeronautics and Astronautics, Nanjing, China, 2015.
19. Lu, W.; Quilitz, M.; Schmidt, H. Nanoscaled BaTiO₃ powders with a large surface area synthesized by precipitation from aqueous solutions: Preparation, characterization and sintering. *J. Eur. Ceram. Soc.* **2007**, *27*, 3149–3159. [[CrossRef](#)]
20. Potdar, H.S.; Deshpande, S.B.; Date, S.K. Chemical coprecipitation of mixed (Ba + Ti) oxalates precursor leading to BaTiO₃ powders. *Mater. Chem. Phys.* **1999**, *58*, S0254–S0584. [[CrossRef](#)]
21. Kumar, V. Solution-precipitation of fine powders of barium titanate and strontium titanate. *J. Am. Ceram. Soc.* **1999**, *82*, 2580–2584. [[CrossRef](#)]
22. Grohe, B.; Miehe, G.; Wegner, G. Additive controlled crystallization of barium titanate powders and their application for thin-film ceramic production: Part I. Powder Synthesis. *J. Mater. Res.* **2001**, *16*, 1901–1910. [[CrossRef](#)]

23. Testino, A.; Buscaglia, M.T.; Buscaglia, V.; Viviani, M. Kinetics and mechanism of aqueous chemical synthesis of BaTiO₃ particles. *Chem. Mater.* **2004**, *16*, 1536–1543. [[CrossRef](#)]
24. Testino, A.; Buscaglia, V.; Buscaglia, M.T.; Viviani, M.; Nanni, P. Kinetic modeling of aqueous and hydrothermal synthesis of barium titanate (BaTiO₃). *Chem. Mater.* **2005**, *17*, 5346–5356. [[CrossRef](#)]
25. Viviani, M.; Buscaglia, M.T.; Testino, A.; Buscaglia, V.; Bowen, P.; Nanni, P. The influence of concentration on the formation of BaTiO₃ by direct reaction of TiCl₄ with Ba(OH)₂ in aqueous solution. *J. Eur. Ceram. Soc.* **2003**, *23*, s0955–s2219. [[CrossRef](#)]
26. Neubrand, A.; Lindner, R.; Hoffmann, P. Room-temperature solubility behavior of barium titanate in aqueous media. *J. Am. Ceram. Soc.* **2000**, *83*, 860–864. [[CrossRef](#)]
27. Hennings, D.F.K.; Metzmacher, C.; Schreinemacher, B.S. Defect Chemistry and microstructure of hydrothermal barium titanate. *J. Am. Ceram. Soc.* **2001**, *84*, 179–182. [[CrossRef](#)]
28. Baudonnet, L.; Pere, D.; Michaud, P.; Grossiord, J.L.; Rodriguez, F. Effect of dispersion stirring speed on the particle size distribution and rheological properties of carbomer dispersions and gels. *J. Disper. Sci. Technol.* **2002**, *23*, 499–510. [[CrossRef](#)]
29. Liang, H.X.; Li, M.Q. Effect of Stirring on formation of spherical xonotlite agglomerates in dynamic hydrothermal process. *Chin. Powder Sci. Technol.* **2002**, *8*, 1–5.
30. Liu, H.Y.; Hu, T.T.; Le, Y.; Chen, J.F. Preparation of micronized ciprofloxacin by reactive precipitation. *J. Beijing Univ. Chem. Technol.* **2008**, *35*, 19–22. [[CrossRef](#)]
31. Zafir, A.V.; Voicu, G.; Jinga, S.I.; Vasile, E.; Lonita, V. Low-temperature synthesis of BaTiO₃ nanopowders. *Ceram. Int.* **2016**, *42*, 1672–1678. [[CrossRef](#)]
32. Li, W.J.; Shi, E.W.; Zhong, W.Z.; Yin, Z.W. Growth mechanism and growth habit of oxide crystals. *J. Cryst. Growth* **1999**, *203*, S0022–S0248. [[CrossRef](#)]
33. Moon, J.; Suvaci, E.; Morrone, A.; Costantino, S.A.; Adair, J.H. Formation mechanisms and morphological changes during the hydrothermal synthesis of BaTiO₃ particles from a chemically modified, amorphous titanium (hydrous) oxide precursor. *J. Eur. Ceram. Soc.* **2003**, *23*, s0955–s2219. [[CrossRef](#)]
34. Pinceloup, P.; Courtois, C.; Vicens, J.; Leriche, A.; Thierry, B. Evidence of a dissolution–precipitation mechanism in hydrothermal synthesis of barium titanate powders. *J. Eur. Ceram. Soc.* **1999**, *19*, s0955–s2219. [[CrossRef](#)]
35. Gao, S.; Li, W. Mechanism of crystal growth. *J. Salt. Lake Res.* **1994**, *2*, 76–80.
36. Zhong, W.Z.; Hua, S.K. Growth units of anion coordination polyhedra and crystal habits. *J. Chin. Ceram. Soc.* **1995**, *33*, 464–470.
37. Shi, E.W.; Yuan, R.L.; Xia, C.T.; Wang, B.G.; Zhong, W.Z. Investigation on the mode of growth unit for hydrothermal synthesis of barium titanate crystallines(II). *ACTA Phys. Sin.* **1997**, *46*, 1–11.
38. Zhong, W.Z.; Xu, G.S.; Luo, H.S.; Hua, S.K. Surface structures dominated by the growth units of anionic coordination polyhedr(III). *J. Synth. Cryst.* **2001**, *30*, 221–226.
39. Chen, J.Z. *Modern Crystal Chemistry*; Science Press: Beijing, China, 2010; pp. 113–123.

